Journal of Power Sources 434 (2019) 226706

Contents lists available at ScienceDirect

Journal of Power Sources

journal homepage: www.elsevier.com/locate/jpowsour

Development of manganese-rich cathodes as alternatives to nickel-rich chemistries

Jason R. Croy [*], Arturo Gutierrez, Meinan He, Bryan T. Yonemoto [1], Eungje Lee, Michael M. Thackeray

Electrochemical Energy Storage Department, Chemical Sciences and Engineering Division, Argonne National Laboratory, Argonne, Illinois, 60439, USA

HIGHLIGHTS

- Mn-rich oxides show promise as competitive alternatives to Ni-rich cathodes.
- Layered-layered-spinel electrodes offer high capacity and good rate capability.
- Novel materials improve interfacial and cycling stability of Mn-rich cathodes.

ARTICLE INFO

Keywords:
Lithium battery
Manganese rich
Layered spinel
Nickel rich
Cathode surface
Manganese dissolution

ABSTRACT

High-energy, inexpensive and safe electrochemistries have been the main goals of lithium-ion battery research for many years. Historically, manganese-based cathodes have long been studied for their attractive cost and safety characteristics [1]. However, due to issues related to both surface and bulk instabilities, manganese-rich electrodes have yet to find substantial success in the high-energy lithium-ion battery market. With current trends in cathode chemistries leaning heavily toward Ni-rich compositions, the factors of cost and safety are again at the forefront of research and development efforts. This paper reports the recent progress made at Argonne National Laboratory (USA) to stabilize manganese-rich cathode structures and surfaces with a specific focus on composite materials with intergrown layered and spinel components; it presents an overview of their electrochemical properties in terms of capacity, energy, and cycle-life in cells with metallic lithium, graphite, and $Li_4Ti_5O_{12}$ anodes. These layered-spinel cathodes show promise as alternatives to highly nickel-rich electrode compositions, which bodes well for continued advances.

1. Introduction

$LiNi_aMn_bCo_cO_2$ oxides, denoted as NMC-abc herein, have attracted considerable attention as promising cathodes for high-energy lithium-ion batteries. In particular, extremely Ni-rich compositions, such as NMC-811, are now being considered for implementation in next-generation electric vehicles. Although such cathodes do indeed hold the promise of yielding cells with significant energy densities, critical issues of safety, cost, and cycle-life have yet to be adequately addressed. While early attempts by researchers and industry have failed in these respects, recent progress has revealed promising Ni-rich NMCs. In fact, Ni-rich compositions such as NMC-622 have now been commercialized. That being said, Ni-rich compositions, especially those beyond ~60% Ni, still face major challenges. Specifically, in order to capitalize fully on the intrinsic energy content of such cathodes in terms of their high capacity and electrochemical potential (vs. Li/Li^+), states of charge (SOCs) above the limits of lattice-oxygen stability must be accessed. In this regard, the term 'high-voltage' might be defined for a particular NMC composition based on this stability limit. For example, Jung et al. have recently shown that the evolution of oxygen from NMC cathodes is triggered in the range ~4.3–4.7 V (vs. Li/Li^+) for compositions from NMC-811 to NMC-111 [2]. Oxygen loss from the cathode surface is not only a safety concern that can lead to dangerous reactions with the electrolyte, but can also result in surface reconstruction, impedance rise, facile transition metal (TM) dissolution, and eventually loss of active lithium in the electrodes [3,4]. This intrinsic, high-voltage limit is clearly composition dependent and must be mitigated or overcome if higher SOCs are to be used during the repeated cycling of a given NMC.

* Corresponding author. Argonne National Laboratory, 9700 South Cass Avenue, Bldg.200, Lemont, IL, 60439-4837, USA.
E-mail address: croy@anl.gov (J.R. Croy).
[1] Current address: Microvast Power Solutions, Inc., Orlando, Fl 32826, USA.

https://doi.org/10.1016/j.jpowsour.2019.226706
Received 18 February 2019; Received in revised form 1 April 2019; Accepted 30 May 2019
Available online 12 June 2019

Alternatives to layered NMCs have been studied for many years and include materials, and derivatives thereof, such as LiM_2O_4 (M = Mn, Ni), $LiFePO_4$, and lithium- and manganese-rich NMCs (LMR-NMC), often denoted in two-component, 'layered-layered' (LL) notation, xLi_2MnO_3•(1-x)$LiNMCO_2$ [5]. LMR-NMCs have received special attention due to the high capacities they can deliver (~250 mAh g^{-1} or more) on repeated cycling [1,6]. However, as with the NMCs discussed above, oxygen sub-lattice instabilities also play an important role. Specifically, for high-capacity LMR-NMCs, an initial charge above ~4.4 V (Li/Li^+) is necessary to access high capacities through an activation process involving oxygen, which triggers structural transitions and the formation of disordered domains within the electrode material. The activated structure continues to evolve with cycling thereby leading to the now well-known phenomena of voltage fade and hysteresis [7–10]. The mechanisms governing the activation process, and hence the activated product, occur as a consequence of local structures within the pristine material in which Li and Mn order preferentially to generate $LiMn_6$ arrangements within the TM layers. The extent of ordering is related to the synthesis temperature and the amount of excess lithium and manganese, x, in the initial xLi_2MnO_3•(1-x)$LiNMCO_2$ composition [11]. As such, it can be shown that the magnitudes of several related phenomena (e.g., partially reversible cation migration, voltage fade, and hysteresis) scale with x [10,11]. In addition, low first-cycle efficiencies, poor rate capability, and high impedance at low SOCs have also been identified as limitations of LMR-NMC electrodes [12]. Despite these challenges, LMR-NMC materials still remain attractive alternatives to Ni-rich NMCs, particularly for transportation applications. Specifically, the cost and safety characteristics of Ni-rich cathodes may be a deciding factor in the need to develop compositions with a higher Mn content, especially if energy and power densities can reach levels comparable to Ni-rich materials. Economically, this may be particularly relevant if a substantial fraction of the lithium-ion market becomes dependent on Ni-rich chemistries, as has been the case for cobalt. This shift to higher Ni-content batteries is currently underway in the electric vehicle market despite concerns that only ~37% of today's nickel supply comes from sulphide mineral ores and less than 10% of that supply is available in battery-grade, nickel-sulfate form [13]. Predictions have been made that only a 10% penetration of the EV market might lead to global nickel supply deficits [13]. Furthermore, Germany, France, China, India, and others have recently proposed to ban the sale of fossil fuel cars in the near future [14]. Optimistically, if these types of policies gain traction, there soon could be no choice but to develop alternative chemistries for such a massive future market. In addition, inexpensive electric vehicles have been identified as a promising economic opportunity for impoverished parts of the world [15]. However, at present, such adoption seems unlikely with respect to the current cost of EV technologies and enabling alternatives could prove critical to such investments.

This report highlights the progress that has been made at Argonne National Laboratory to develop Mn-rich cathodes capable of competing with Ni-rich counterparts. A bottom-up approach to fabricate lithium-rich cathodes is taken whereby x, in xLi_2MnO_3•(1-x)$LiNMCO_2$ 'layered-layered' (LL) electrodes, is limited to less than ~0.25 and the composition modified by reducing the lithium content slightly to integrate spinel domains in the LMR-NMC structure, thereby creating composite, 'layered-layered-spinel' (LLS) structures with a Mn content of ~50% [16,17]. This approach represents a comprehensive strategy to address the limitations of LMR-NMCs by:

1) Inherently limiting the extent of Li/Mn ordering (i.e., $x < 0.25$) and, therefore, damaging effects (e.g., voltage fade) of the electrochemical activation process whereby lithium and oxygen are removed from the Li_2MnO_3 component, while still allowing for substantial capacities (>200 mAh g^{-1});
2) Introducing spinel domains (especially at surfaces) to help improve rate capability and stability; and
3) Introducing vacant lithium sites, by way of the spinel component, that can take up lithium on the first discharge after the activation of the Li_2MnO_3 component, thereby reducing first-cycle, irreversible capacities.

Because local structures within LMR-NMCs dictate macroscopic electrode behavior, as is recently being understood [10,18,19], engineering the nano-scale domain structure through incorporation of spinel and "spinel-like" components may contribute to the unique properties and/or relative stabilization of LLS cathodes. When combined with efforts to stabilize cathode surfaces through both surface treatments and electrolyte formulations, the strategy reported here shows promise for developing Mn-rich cathodes that can compete with their Ni-rich counterparts in terms of cost, safety and electrochemical performance. A comparison of the electrochemical performance of a selected LLS electrode composition ('LLS-352') in cells with metallic lithium, $Li_4Ti_5O_{12}$, and graphite anodes is made with its Ni-rich counterpart NMC-532.

2. Experimental

LLS particles were synthesized from TM carbonate precursors made by co-precipitation of Mn-, Ni-, and Co-sulfates. A baseline LLS electrode composition, derived from the LL compound $0.25Li_2MnO_3$•$0.75LiMn_{0.375}Ni_{0.375}Co_{0.25}O_2$ by reducing the lithium content to target a 15% spinel content, was selected based on previous characterization and electrochemical studies [17,18]. This material is denoted LLS-352 for convenience to designate the more accurate Ni:Mn:Co ratio of 0.28:0.53:0.19. Details of the synthesis and characterization of these, and other LLS compositions, can be found in references 16 and 20. Commercially available NMC-532 (Toda America) with a higher nickel and lower manganese content was used as the NMC standard for comparison. Cathode powders were surface-treated by typical wet-synthesis procedures in an aqueous solution of Li_2WO_4, $Al(NO_3)_3{\cdot}9H_2O$, and NH_4F (~3:1:1, referred to herein as WAlF) followed by drying and annealing at 550 °C in air for 6 h. LLS-352 powders were also surface treated in aqueous solutions of $Al(NO_3)_3{\cdot}9H_2O$ (0.5 wt%) only, followed by drying at ~110 °C overnight without subsequent annealing. Details of these coatings can be found elsewhere [21,22].

Electrochemical cycling tests were carried out in 2032-type coin cells with cathode laminate formulations of 84:8:8: (oxide:PVDF binder:carbon). Lithium-metal, $Li_4Ti_5O_{12}$, or graphite mixed with C-45 carbon and PVDF binder (graphite:C-45: PVDF = 92:2:6) anodes were used, as noted in the text. Negative to positive electrode capacity ratios were kept in the range of 1.1–1.5 such that the capacity of the cells was always cathode limited. The electrolytes used in the cells were either 1.2 M $LiPF_6$ in EC: EMC (3:7 by weight), hereafter referred to as the Gen2 electrolyte, or a newly-developed fluorinated formulation consisting of 1.0 M $LiPF_6$ in DFEC/FEMC (3:7 by weight). Cells were cycled at a constant current density, typically ~15 mA g^{-1} at 30 °C, unless otherwise specified.

3. Results and discussion

3.1. A comparison of baseline LLS-352//Li vs. NMC-532//Li cells

Fig. 1a shows a plot of discharge capacity as a function of cycle number for coin cells with WAlF-coated LLS-352 and NMC-532 cathodes and Li metal anodes. The LLS-352 electrode was electrochemically activated on the initial charge/discharge cycle between 4.6 and 2.0 V with subsequent cycling between 4.45 and 2.5 V, whereas the standard NMC-532 electrode was only cycled between 4.45 and 2.5 V. Both electrodes show excellent capacity retention for 50 cycles. This comparative test highlighted several attractive features and advantages of the LLS-352 electrode. First, the coulombic efficiency of the electrode during the initial activation cycle (~96%) is significantly higher than that of the NMC-532 electrode (~88%) – a consequence of the

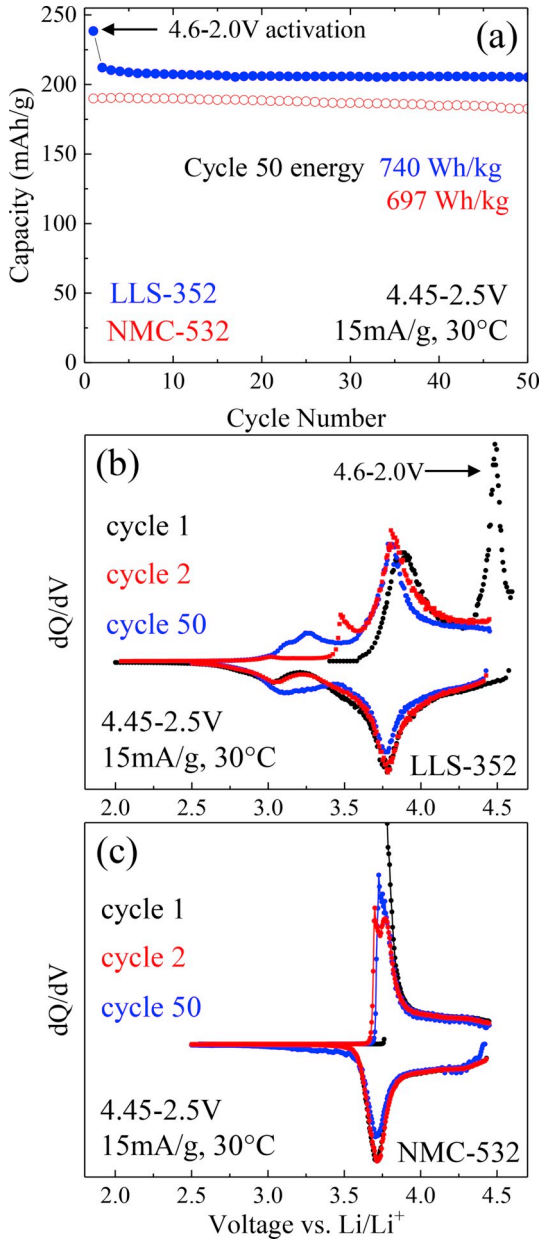

Fig. 1. (a) Capacity vs. cycle number plots for lithium cells with LLS-352 and NMC-532 electrodes. (b) and (c) Corresponding dQ/dV plots of the data in (a). Ageing cycles were between 4.45 and 2.5 V. The LLS also underwent a first cycle activation between 4.6 and 2.0 V.

incorporation of a spinel component, as previously reported [16,17], and a more robust surface compared to a pristine LLS that was generated by the WAlF treatment. Fig. 1(b) and (c) show the corresponding dQ/dV plots of the cells containing the LLS-352 and NMC-532 electrodes, respectively. The sharp peak at 4.6 V in Fig. 1b on the first cycle of the LLS-352//Li cell is indicative of the activation of the compositionally-modified $0.25Li_2MnO_3 \bullet (1\text{-}x)LiMn_{0.375}Ni_{0.375}Co_{0.25}O_2$ component of the LLS electrode, during which a substantial amount of Li was extracted (~250 mAh g^{-1} in total for the first charge), consistent with earlier reports [16,17,20]. It is remarkable how the incorporation of a small amount of spinel (15% or less) within the electrode structure can improve the first-cycle efficiency of the cell so significantly. A second advantage is that the voltage fade phenomenon that leads to capacities in the ~3.0–3.5 V region is substantially less pronounced than it is when LL electrode structures with higher amounts of excess lithium and manganese (>30%) and without a spinel component are used [11].

In this instance, the LLS-352 electrode delivers virtually all its capacity above 2.8 V, even on the 50th cycle (Fig. 1b). Of particular significance is that on the 50th cycle, the energy density of the LLS-352//Li cell, based on the mass of the active metal oxide electrode only, 740 Wh kg^{-1}_{oxide}, is still greater than that of the NMC-532//Li cell (697 Wh kg^{-1}_{oxide}), both of which include the capacity contribution from the region of voltage fade.

Fig. 2 shows a plot of discharge energy (Wh kg^{-1}_{oxide} only) vs. discharge rate for lithium cells with WAlF surface-treated LLS-352 and NMC-532 cathodes. At slow rates, even when the NMC-532//Li cell is charged to 4.6 V (first cycle), the LLS-352//Li cell has a clear advantage in terms of specific energy (Wh kg^{-1}_{oxide}). As the discharge rate increases, the NMC-532//Li and LLS-352//Li cells deliver similar energies until rates between 1 and 2C are reached. Above 2C, the NMC-532 electrode shows a marginally superior performance delivering ~550 Wh kg^{-1}_{oxide} at a 9.74C rate. Note that the electrode loadings in each case were low (~6 mg/cm^2) and that the testing was conducted at the beginning of life for both cells. This was done intentionally in order to better understand the capabilities of the electrode materials themselves rather than electrode-level properties – a topic presented in more detail below. Nevertheless, it is clear from Figs. 1 and 2 that the lithium- and manganese-rich LLS-352 electrode selected for this investigation possesses attractive characteristics when compared to a conventional, commercially available NMC-532 material, particularly in terms of energy and rate.

3.2. LLS-352//$Li_4Ti_5O_{12}$ cells

$Li_4Ti_5O_{12}$ (LTO) is an anode of significant interest for lithium-ion battery applications [23]. Although it offers a higher potential (1.55 V vs. Li/Li^+) than lithiated graphite (~0.1 V vs. Li/Li^+), thereby lowering the cell voltage, a LTO anode is attractive in terms of its structural stability to lithium insertion and extraction and to enhancing the safety and power attributes of lithium-ion cells. In addition, because LTO operates at 1.55 V vs. Li/Li^+, aluminum instead of copper can be used as the current collector and Li–Al alloying reactions can be avoided. Therefore, in order to assess the long-term stability of the LLS electrode in a more stable environment, LLS-352//LTO cells were evaluated. Fig. 3 shows capacity vs. cycle number plots of two duplicate cells in which the surface of the LLS-352 electrode had been subjected to a

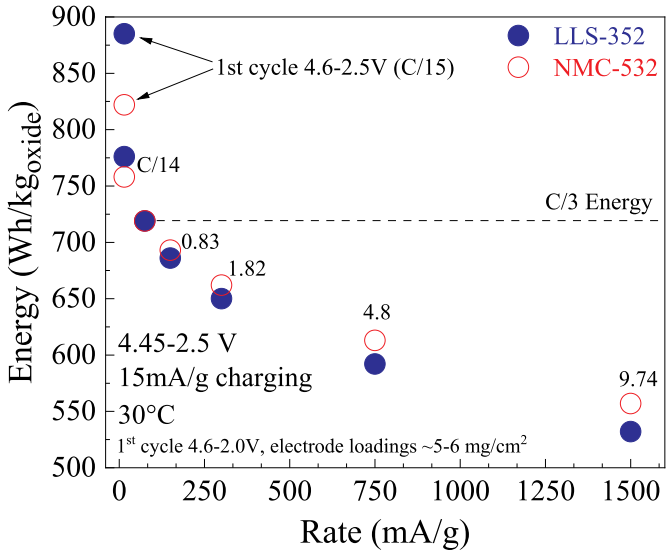

Fig. 2. Plot of discharge energy (Wh kg^{-1}_{oxide} only) vs. discharge rate for lithium cells with WAlF surface-treated LLS-352 and NMC-532 cathodes. The charging current was kept constant while the discharge rate was varied from C/15 to 9.74C, as indicated. Cells were cycled between 4.6 and 2.0 V on the first cycle and subsequently between 4.45 and 2.5 V.

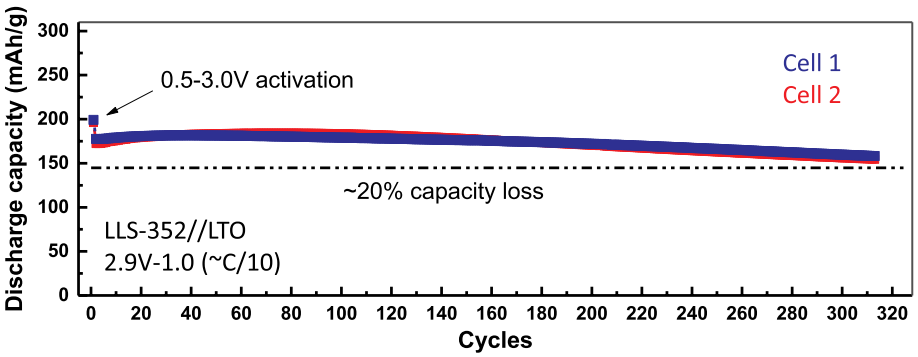

Fig. 3. Discharge capacity (cathode) vs. cycle number plots of duplicate LLS-352//Gen2//LTO cells. 20% capacity loss is based on the average discharge capacity of ~180 mAh g^{-1} obtained on cycle 20. Duplicate cells shown for reproducibility.

low-temperature (~110 °C) Al-coating process [22]. Cells underwent a first-cycle activation between 3.0 and 0.5 V (i.e., between ~4.55 and 2.05 V vs. Li/Li^+) followed by ageing cycles between 2.9 and 1.0 V (~C/10).

The end-of-life yardstick, which is typically when there is a 20% capacity loss of the maximum discharge capacity, is indicated by the dashed line on the plot in Fig. 3. The second-cycle average discharge capacity was 176 mAh g^{-1} and the maximum average capacity was 183 mAh g^{-1}, revealing a modest, continued activation over the early cycles. The cell delivered a cathode capacity of more than 160 mAh g^{-1} for >300 cycles with >85% capacity retention, highlighting its steady electrochemical reversibility.

3.3. LLS-352//graphite cells

One of the biggest concerns about NMC electrode materials is the dissolution of the transition metal ions in the electrolyte and their subsequent deposition and reduction at graphitic anodes, which can deleteriously affect the electrochemical performance of lithium-ion cells. TM dissolution/deposition phenomena have been identified as major contributors to the loss of active lithium in NMC//graphite cells, which has been shown to be most acute for manganese relative to nickel and cobalt [24,25]. (Note that lithium-ion cells with LTO anodes, as described above, do not suffer as severely from TM dissolution, deposition and reduction because LTO is significantly less reactive than lithiated-graphite anodes; it operates well above the potential of lithiated graphite and also above the reduction potential of the organic electrolyte solvents.) TM dissolution and its effect on graphitic anodes have therefore been the topic of considerable ongoing research and debate. It is clear that whatever the underlying mechanisms are, TM dissolution in NMC//graphite cells still requires further attention to circumvent this critical issue.

Fig. 4 shows electrochemical data for three LLS-352//graphite cells with 1) an untreated baseline LLS-352 electrode, 2) an Al-treated LLS-352 electrode, and 3) an Al-treated LLS electrode and a 0.5% LiDFOB electrolyte additive. The cycling protocol was developed under the Department of Energy's Deep Dive project, *Enabling High-Energy/High-Voltage Cathodes*. This protocol is intended to exacerbate and accelerate degradation effects at high voltage such as TM dissolution; it was also established to provide information on important metrics such as impedance rise with cycling and to offer a standard procedure that researchers across institutions could use reliably to make one-to-one comparisons about the performance of new or modified materials (cathodes, anodes, electrolytes, additives, coatings …) within a given system. Details of the Deep Dive program and protocol can be found in reference 26.

Under the aggressive protocol used (i.e., 4.4–2.5 V cycling vs. graphite, C/2 ageing cycles, and a 3-h hold at the top of each charge) the baseline cell with an untreated LLS-352 electrode lost almost 50% of its

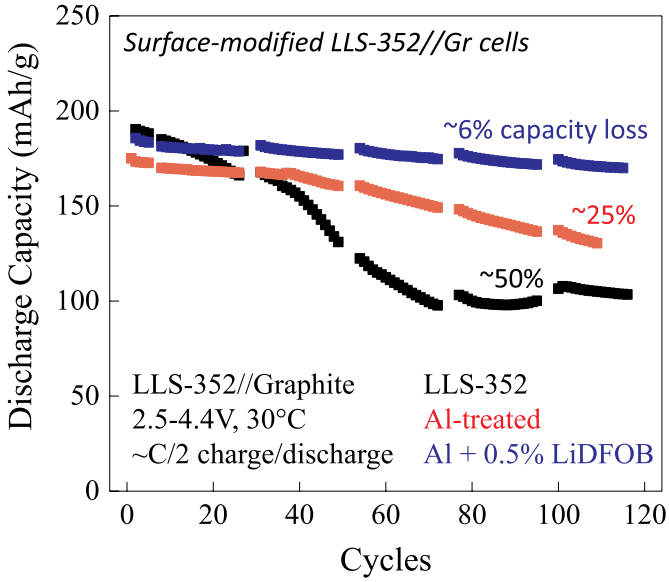

Fig. 4. Capacity vs. cycle number plots of three LLS-352//Gen2//graphite cells containing 1) an untreated LLS-352 electrode, 2) an Al-treated LLS-352 electrode, and 3) an Al-treated LLS electrode with a 0.5% LiDFOB additive. The cycling protocol is described in reference 26.

capacity after 75 cycles. In comparison, the cell with an Al-surface-treated LLS-352 electrode lost only ~25% of its capacity after ~120 cycles (Fig. 4). When the additive, lithium difluoro (oxalate)borate (LiDFOB) [27], was added (0.5% weight percent) to the Gen2 electrolyte, a further improvement in cell performance was observed. In this case, the high capacity and cycling stability of the electrode during the first few cycles mimicked that of the baseline electrode, generating >180 mAh g^{-1}, whereas some capacity (~170 mAh g^{-1}) was sacrificed by the Al-surface-treated LLS-352 electrode in a cell without the additive. Note that the addition of the additive enhances the cycling stability of the cell such that there is only a 6% capacity loss over the 120 cycles on test. Fig. 4 shows that Al-treatment of the LLS-352 electrode alone, i.e., no additive, is not as effective as using a combination of both Al-surface-treatment and the LiDFOB additive. Likewise, cells with 0.5% LiDFOB additive alone, i.e., without Al-treatment of the LLS-352 (data not provided), showed slightly lower coulombic efficiencies and a higher impedance rise on cycling than using a combination of both Al-surface-treatment and the LiDFOB additive.

3.4. Area specific impedance

Fig. 5 shows area specific impedance (ASI, ohm•cm^2) data for the

three cell configurations presented in Fig. 4. The data were calculated from hybrid-pulse-power-characterization (HPPC) cycles, implemented every 20 cycles (shown as breaks in the cycling data of Fig. 4), as detailed in Long et al. [26] The impedance of the baseline cell, as monitored by the HPPC test, increases dramatically from approximately 50 Ω cm^2 at mid-discharge after 7 cycles to reach a final value of ~250 Ω cm^2 after 99 cycles (Fig. 5a), while the cell with an Al-treated LLS-352 electrode showed an approximate 35% improvement in the net impedance rise, reaching ~165 Ω cm^2 at the end of the test (Fig. 5b). In stark contrast, however, the impedance data of a cell with an Al-treated LLS-352 electrode and the LiDFOB electrolyte additive show two remarkable results (Fig. 5c). First, the initial impedance of these cells is only ~25–30 Ω cm^2, considerably lower than that of the baseline cell (~50 Ω cm^2) and more on par with layered NMCs such as NMC-532 (~20 Ω cm^2). Second, the impedance rise measured over ~100 cycles is negligible after the addition of only 0.5% LiDFOB to the Gen2 electrolyte. Previous studies have already shown that LiDFOB can improve the capacity retention of Li–Mn rich cathodes [27]; however, in these reports, much higher amounts of LiDFOB (~4x) were typically needed to improve capacity retention and resulted in lower coulombic efficiency. Our results emphasize that the unique combination of a low-temperature Al treatment and the addition of just 0.5% LiDFOB dramatically improves the interfacial stability of a LLS-352 electrode. In this respect, we note that 'layered-layered' LMR-NMC electrodes have been reported to exhibit a poor impedance at low SOCs, for example, below ~3.3 V [12], while our experiments only probe the SOC of the electrodes to 3.3 V and above. Studies at Argonne National Laboratory are ongoing to understand the unique component of ASI at lower SOCs for these materials. An added point of interest is that Al-treatment, when conducted at lower temperatures, e.g. ~110 °C, does not show the same benefit on nickel-rich NMC-532 electrodes as it does on Mn-rich LLS-352 electrodes [22], emphasizing the importance of cathode composition with respect to the application of specific surface-stabilization strategies.

3.5. LLS with fluorinated electrolyte

Clearly, from the data presented above, surface-treated LLS-352 particles enable high first-cycle efficiencies, high cycling capacities and energies at tenable voltages (4.4 vs. graphite), and a good rate capability. Furthermore, good electrochemical stability under aggressive cycling protocols was demonstrated. A next logical step for further improvement is to discover and develop new, advanced electrolytes. Several studies have alluded to the potential benefits of using fluorinated systems to stabilize the surface of metal oxide electrode particles [28,29]. Recent efforts at Argonne National Laboratory to develop novel, fluorinated electrolyte formulations have shown promise for stabilizing both cathode and anode surfaces at high and low electrochemical potentials, respectively. In particular, a unique ability to pre-form an extremely robust SEI layer on an anode surface, such as graphite, has been developed, the details of which are reported elsewhere [30].

In this study, we have evaluated the performance of cells having a graphite anode with a pre-formed SEI and an untreated LLS-352 cathode, in the absence of any coating or electrolyte additive, under high-voltage cycling. Fig. 6 shows a discharge capacity (left axis) and coulombic efficiency (right axis) vs. cycle number plot for such a cell when cycled between 4.5 and 2.5 V at a ~C/10 current rate. The graphite anode was first pre-formed, electrochemically, during one charge/discharge cycle in a Li//graphite cell using a 1.0 M $LiPF_6$ in DFEC/FEMC (3:7 wt) electrolyte to form a stable SEI on the graphite electrode. Thereafter, new cells were assembled using the pre-formed graphite anode, a LLS-352 cathode, and fresh DFEC/FEMC electrolyte. These pre-formed anodes can also be used to overcome first-cycle inefficiencies associated with electrolyte reduction at the graphite surface, which can be large for fluorinated formulations [30]. The primary reason for this aspect of our study was not only to probe the long-term stability of the pre-formed graphite electrode but also to monitor the electrochemical stability of the LLS-352 particle surface in the DFEC/FEMC electrolyte. From this standpoint, Fig. 6 clearly illustrates that a LLS-352//DFEC/FEMC//preformed graphite cell delivers excellent cycling capacity and stability. Specifically, the LLS-352 electrode delivers an impressive 225 mAh g^{-1} over the 100 cycles on test with little capacity fade and high efficiency. The average energy delivered over the 100 cycles on test, at the ~C/10 rate, for this LLS electrode vs. graphite was approximately 800 Wh kg^{-1}_{oxide} (Fig. 7). The cell suffered ~10% energy fade over the 100 cycles, that was attributed predominantly to the voltage fade of the 'layered-layered' component in the lithium- and manganese-rich LLS-352 electrode.

4. Conclusions

This study has emphasized several symbiotic strategies to enable the use of Mn-rich NMC electrode compositions as alternatives to Ni-rich systems in lithium-ion cells. Specifically, it has been demonstrated that Mn-rich LLS materials, such as LLS-352, can be synthesized to yield high-capacity, high-energy cathodes with properties on par with their nickel-rich counterparts such as NMC-532. Furthermore, it has been shown that by implementing surface stabilization strategies particularly suited to Li- and Mn-rich compositions, long-term cycling stability can be achieved in full-cell configurations using graphite anodes, even under high-voltage (4.5 V vs. graphite) operation. The results are encouraging and show promise for overcoming the barriers that are currently stalling the entry of Mn-rich cathodes in the lithium-ion battery market. Further advances to LLS electrode composition and performance improvements can therefore be expected. Efforts are currently underway at Argonne National Laboratory to monitor and improve the ASI of cells with LLS electrodes at low SOCs and to synthesize and identify precursors with a

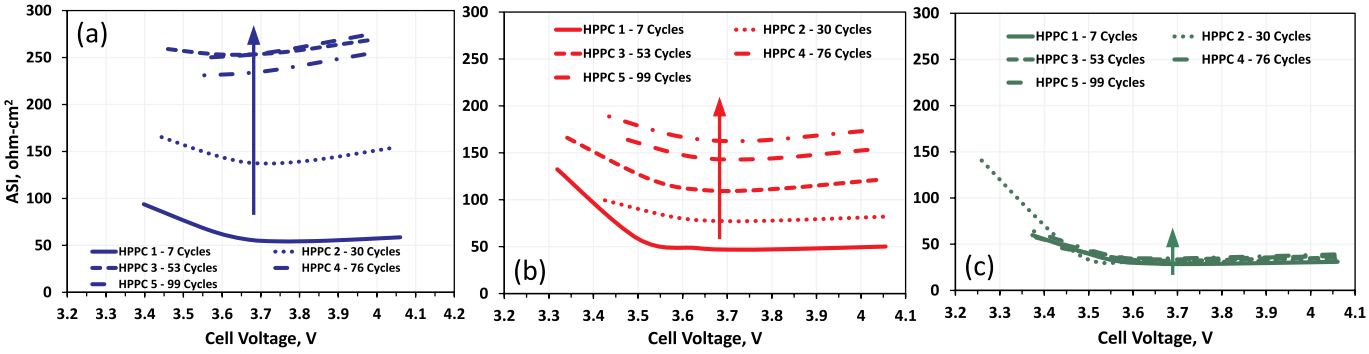

Fig. 5. Area specific impedance (ASI, ohm•cm [2]) data for LLS-352//Gen2//graphite cells containing (a) untreated LLS-352, (b) Al-treated LLS-352, and (c) Al-treated LLS-352 plus 0.5% LiDFOB additive.

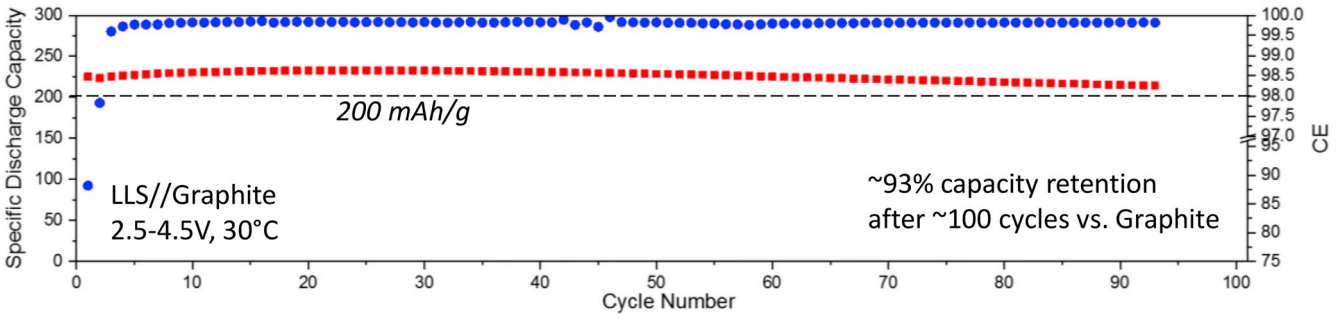

Fig. 6. Discharge capacity (left axis, red squares) and coulombic efficiency (right axis, blue circles) vs. cycle number plot of a LLS-352//graphite cell with a graphite anode pre-formed in DFEC/FEMC electrolyte. (For interpretation of the references to colour in this figure legend, the reader is referred to the web version of this article.)

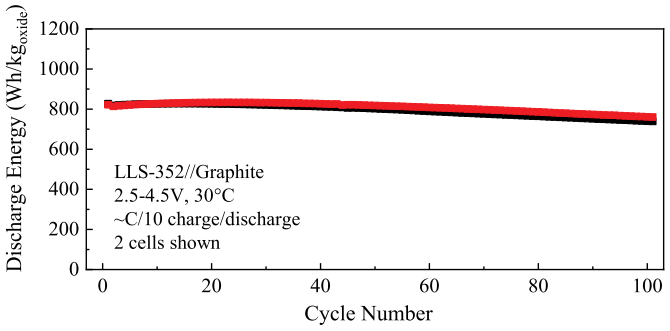

Fig. 7. Discharge energy (Wh kg^{-1}_{oxide}) delivered at a ~C/10 rate for LLS-352// graphite cells with preformed graphite anodes in a DFEC/FEM electrolyte after reference 30. Data for two cells, highlighting the reproducibility of the test, are provided.

lower cobalt content and a higher tap-density to maximize cost benefits and volumetric energy densities. In addition, the thermal properties of LLS electrodes, which have not been reported herein, in combination with various treatments and electrolytes, are under investigation. The results of these studies will be reported elsewhere.

Acknowledgments

Support from the U.S. Department of Energy, Office of Energy Efficiency and Renewable Energy, in particular David Howell and Peter Faguy, is gratefully acknowledged. The submitted manuscript has been created by UChicago Argonne, LLC, Operator of Argonne National Laboratory ("Argonne"). Argonne, a U.S. Department of Energy Office of Science Laboratory, is operated under Contract No. DE-AC02-06CH11357. The U.S. Government retains for itself, and others acting on its behalf, a paid-up nonexclusive, irrevocable worldwide license in said article to reproduce, prepare derivative works, distribute copies to the public, and perform publicly and display publicly, by or on behalf of the Government.

References

[1] M.M. Thackeray, J.R. Croy, E. Lee, A. Gutierrez, M. He, J.S. Park, B.T. Yonemoto, B.R. Long, J.D. Blauwkamp, C.S. Johnson, Y. Shin, W.I.F. David, The quest for manganese-rich electrodes for lithium batteries: strategic design and electrochemical behavior, Sustain. Energy Fuels 2 (2018) 1375.

[2] R. Jung, M. Metzger, F. Maglia, C. Stinner, H.A. Gasteiger, *Oxygen Release and its Effect on the cycling Stability of $LiNi_xMn_yCo_zO_2$ (NMC) cathode Materials for Li-ion batteries*, J. Electrochem. Soc. 164 (2017) A1361–A1377.

[3] N.V. Faenza, Z.W. Lebens-Higgins, P. Mukherjee, S. Sallis, N. Pereira, F. Badway, A. Halajko, G. Ceder, F. Cosandey, L.F.J. Piper, G.G. Amatucci, *Electrolyte-induced surface Transformation and transition-metal Dissolution of fully delithiated $LiNi_{0.8}Co_{0.15}Al_{0.05}O_2$*, Langmuir 33 (2017) 9333–9353.

[4] J.A. Gilbert, J. Bareno, T. Spila, S.E. Trask, D.J. Miller, B.J. Polzin, A.N. Jansen, D. P. Abraham, Cycling behavior of NCM523/graphite lithium-ion cells in the 3-4.4 V range: diagnostic studies of full cells and harvested electrodes, J. Electrochem. Soc. 164 (2017) A6054–A6065.

[5] C.S. Johnson, J.S. Kim, C. Lefief, N. Li, J.T. Vaughey, M.M. Thackeray, *The significance of the Li_2MnO_3 component in 'composite' $xLi_2MnO_3•(1-x)LiMn_{0.5}Ni_{0.5}O_2$ electrodes*, Electrochem. Commun. 6 (2004) 1085–1091.

[6] T. Ohzuku, M. Nagayama, K. Tsuji, K. Ariyoshi, High-capacity lithium insertion materials of lithium nickel manganese oxides for advanced lithium-ion batteries: toward rechargeable capacity more than 300 mA h g(-1), J. Mater. Chem. 21 (2011) 10179–10188.

[7] J.R. Croy, K.G. Gallagher, M. Balasubramanian, Z.H. Chen, Y. Ren, D. Kim, S. H. Kang, D.W. Dees, M.M. Thackeray, *Examining Hysteresis in Composite $xLi_2MnO_3•(1-x)LiMO_2$ cathode structures*, J. Phys. Chem. C 117 (2013) 6525–6536.

[8] J.R. Croy, D. Kim, M. Balasubramanian, K. Gallagher, S.H. Kang, M.M. Thackeray, *Countering the voltage Decay in high Capacity $xLi_2MnO_3•(1-x)LiMO_2$ electrodes (M=Mn, Ni, Co) for Li^+-Ion batteries*, J. Electrochem. Soc. 159 (2012) A781–A790.

[9] K.G. Gallagher, J.R. Croy, M. Balasubramanian, M. Bettge, D.P. Abraham, A. K. Burrell, M.M. Thackeray, Correlating hysteresis and voltage fade in lithium- and manganese-rich layered transition-metal oxide electrodes, Electrochem. Commun. 33 (2013) 96–98.

[10] J.R. Croy, M. Balasubramanian, K.G. Gallagher, A.K. Burrell, Review of the US department of energy's "Deep dive" effort to understand voltage fade in Li- and Mn-rich cathodes, Acc. Chem. Res. 48 (2015) 2813–2821.

[11] J.R. Croy, K.G. Gallagher, M. Balasubramanian, B.R. Long, M.M. Thackeray, *Quantifying Hysteresis and voltage Fade in $xLi_2MnO_3•(1-x)LiMn_{0.5}Ni_{0.5}O_2$ Electrodes as a Function of Li_2MnO_3 content*, J. Electrochem. Soc. 161 (2014) A318–A325.

[12] S.R. Gowda, D.W. Dees, A.N. Jansen, K.G. Gallagher, Examining the electrochemical impedance at low states of charge in lithium- and manganese-rich layered transition-metal oxide electrodes, J. Electrochem. Soc. 162 (2015) A1374–A1381.

[13] Visual Capitalist. http://www.visualcapitalist.com/nickel-secret-driver-battery-revolution/.

[14] Quartz. https://qz.com/1341155/nine-countries-say-they-will-ban-internal-combustion-engines-none-have-a-law-to-do-so/.

[15] C.M. Christensen, E. Ojomo, K. Dillon, The Prosperity Paradox, Harper Business, 2019.

[16] B.R. Long, J.R. Croy, J.S. Park, J.G. Wen, D.J. Miller, M.M. Thackeray, *Advances in stabilizing 'Layered-Layered' $xLi_2MnO_3•(1-x)LiMO_2$ (M=Mn, Ni, Co) Electrodes with a spinel component*, J. Electrochem. Soc. 161 (2014) A2160–A2167.

[17] D. Kim, G. Sandi, J.R. Croy, K.G. Gallagher, S.-H. Kang, Eungje Lee, M.D. Slater, C. S. Johnson, M.M, Thackeray *composite 'Layered-Layered-Spinel' cathode Strcutures for lithium-ion batteries*, J. Electrochem. Soc. 160 (2013) A31–A38.

[18] M. Saubanere, E. McCalla, J.M. Tarascon, M.L. Doublet, The intriguing question of anionic redox in high-energy density cathodes for Li-ion batteries, Energy Environ. Sci. 9 (2016) 984–991.

[19] H. Iddir, J.R. Croy, K.G. Gallagher, C.S. Johnson, R. Benedek, M. Balasubramanian, First-charge instabilities of layered-layered lithium-ion-battery materials, Phys. Chem. Chem. Phys. 17 (2015) 24382–24391.

[20] J. Croy, J.S. Park, Y. Shin, B. Yonemoto, M. Balasubramanian, B. Long, Y. Ren, M. Thackeray, Prospects for spinel-stabilized, high-capacity lithium-ion battery cathodes, J. Power Sources 334 (2016) 213–220.

[21] Croy, J. R.; Balasubramanian, M.; Park, J.-S. High Valent Lithiated Surface Structures for Lithium Ion Battery Electrode Materials. U.S. Patent Pub. No.: 20190013518 2019.

[22] Croy, J. R.; Gutierrez, A.; Thackeray, M. M.; He, M. Surface Treatment for Lithium Battery Electrode Materials. U.S. Patent Pub. No.: 20180254483 2018.

[23] X. Sun, P.V. Radovanovic, B. Cui, *Advances in spinel $Li_4Ti_5O_{12}$ anode materials for lihtium-ion batteries*, New J. Chem. 39 (2015) 38–63.

[24] R. Jung, F. Linsenmann, R. Thomas, J. Wandt, S. Solchenbach, F. Maglia, C. Stinner, M. Tromp, H.A. Gasteiger, Nickel, Manganese, and cobalt dissolution from Ni-rich NMCS and their effects on NMC622-graphite cells, J. Electrochem. Soc. 166 (2019) A378–A389.

[25] J.A. Gilbert, I.A. Shkrob, D.P. Abraham, Transition metal dissolution, ion migration, electrocatalytic reduction and capacity loss in lithium-ion full cells, J. Electrochem. Soc. 164 (2017) A389–A399.

[26] B.R. Long, S.G. Rinaldo, K.G. Gallagher, D.W. Dees, S.E. Trask, B.J. Polzin, A. N. Jansen, D. Abraham, I. Bloom, J. Bareno, J.R. Croy, Enabling high-energy, high-voltage lithium-ion cells: stadardization of coin-cell assembly, electrochemical testing, and evaluation of full cells, J. Electrochem. Soc. 163 (2016) A2999–A3009.
[27] Y. Zhu, Y. Li, M. Bettge, D.P. Abraham, Positive electrode passivation by LiDFOB electrolyte additive in high-capacity lithium-ion cells, J. Electrochem. Soc. 159 (2012) A2109–A2117.
[28] A. Tornheim, S. Sharifi-Asl, J.C. Garcia, J. Bareno, H. Iddir, R. Shahbaxian-Yassar, Z. Zhang, Effect of electrolyte composition on rocksalt surface degradation in NMC cathodes durin high-voltage potentiaostatic holds, Nanomater. Energy 55 (2019) 216–225.
[29] Z. Zhang, L. Hu, H. Wu, W. Weng, M. Koh, P.C. Redfern, L.A. Curtiss, K. Amine, Fluorinated electrolytes for 5 V lithium-ion battery chemistry, Energy Environ. Sci. 6 (2013) 1806.
[30] A. Tornheim, R. Sahore, M. He, J.R. Croy, Z.C. Zhang, Preformed anodes for high-voltage lithium-ion battery performance: fluorinated electrolytes, crosstalk, and the origins of impedance rise, J. Electrochem. Soc. 165 (2018) A3360–A3368.